Supporting Information

van Rooij *et al.* 10.1073/pnas.0805038105

SI Materials and Methods

Surgical Procedures. All animal protocols were approved by the Institutional Animal Care and Use Committee of the University of Texas Southwestern Medical Center. Adult C57Bl6 male mice were anesthetized with 2.4% isoflurane and placed in a supine position on a heating pad (37°C). Animals were intubated with a 19G stump needle and ventilated with room air, using a MiniVent mouse ventilator (Hugo Sachs Elektronik; stroke volume, 250 μl, respiratory rate, 210 breaths per minute). Via left thoracotomy between the fourth and fifth ribs, the left anterior coronary artery (LCA) was visualized under a microscope and ligated by using a 6–0 prolene suture. Regional ischemia was confirmed by visual inspection under a dissecting microscope (Leica) by discoloration of the occluded distal myocardium. Sham operated animals underwent the same procedure without occlusion of the LCA.

Histological Analysis and RNA *in Situ* Hybridization. Tissues used for histology were incubated in Krebs-Henselheit solution, fixed in 4% paraformaldehyde, sectioned, and processed for H&E and Masson's Trichrome staining or *in situ* hybridization by standard techniques (1).

Microarray for miRNAs. Microarray assay was performed by using a service provider (LC Sciences). The assay started from 10 μg of total RNA sample, which was size fractionated by using a YM-100 Microcon centrifugal filter (from Millipore) and the small RNAs (< 300 nt) isolated were 3′-extended with a poly(A) tail, using poly(A) polymerase. An oligonucleotide tag was then ligated to the poly(A) tail for later fluorescent dye staining; two different tags were used for the two RNA samples in dual-sample experiments. Hybridization was performed overnight on a μParaflo microfluidic chip, using a microcirculation pump (Atactic Technologies) (2). On the microfluidic chip, each detection probe consisted of a chemically modified nucleotide coding segment complementary to target microRNA (from miRBase, http://microrna.sanger.ac.uk/sequences) or other RNA (control or customer defined sequences) and a spacer segment of polyethylene glycol to extend the coding segment away from the substrate. The detection probes were made by *in situ* synthesis using PGR (photogenerated reagent) chemistry. The hybridization melting temperatures were balanced by chemical modifications of the detection probes. Hybridization used 100 μl of 6xSSPE buffer [0.90 M NaCl, 60 mM Na_2HPO_4, 6 mM EDTA (pH 6.8)] containing 25% formamide at 34°C. After RNA hybridization, tag-conjugating Cy3 and Cy5 dyes were circulated through the microfluidic chip for dye staining. Fluorescence images were collected by using a laser scanner (GenePix 4000B; Molecular Devices) and digitized by using Array-Pro image analysis software (Media Cybernetics). Data were analyzed by first subtracting the background and then normalizing the signals, using a locally weighted regression (LOWESS) filter (3). For two-color experiments, the ratio of the two sets of detected signals (log2 transformed, balanced) and P values of the t test were calculated; differentially detected signals were those with <0.01 P values.

Cell Culture, Transfection, and Luciferase Assays. Cardiac fibroblasts (CFs) were isolated as described in ref. 4. Briefly, hearts were excised from anesthetized neonatal 1 to 2-day-old Sprague–Dawley rats (Harlan Sprague–Dawley), minced, and digested with pancreatin 0.1%. Cells were plated on primaria plates for 2 h, and the medium that contained the cardiomyocyte fraction of the digested tissue was removed. Cardiac fibroblasts attached and proliferated much more rapidly than cardiac myocytes; this produced virtually pure fibroblast cultures after the first passage, which was confirmed by repeated differential plating and microscopic evaluation. Cells were detached with 0.05% trypsin for passaging, and culture studies were performed at passages 2 to 4. Cells were grown in high glucose (4.5 gm/lt) DMEM containing 10% heat-inactivated FBS and antibiotics (penicillin and streptomycin). Myofibroblast differentiation was induced by changing the medium to low serum (2% FBS) with L-ascorbic acid (10 μg/ul) and administration of 10 ng/ml TGFβ1 for 48 h.

1. Shelton JM, Lee MH, Richardson JA, Patel SB (2000) Microsomal triglyceride transfer protein expression during mouse development. *J Lipid Res* 41:532–537.
2. Gao X, Gulari E, Zhou X (2004) In situ synthesis of oligonucleotide microarrays. *Biopolymers* 73:579–596.
3. Bolstad BM, Irizarry RA, Astrand M, Speed TP (2003) A comparison of normalization methods for high density oligonucleotide array data based on variance and bias. *Bioinformatics* 19:185–193.
4. Simpson P, Savion S (1982) Differentiation of rat myocytes in single cell cultures with and without proliferating nonmyocardial cells. Cross-striations, ultrastructure, and chronotropic response to isoproterenol. *Circ Res* 50:101–116.

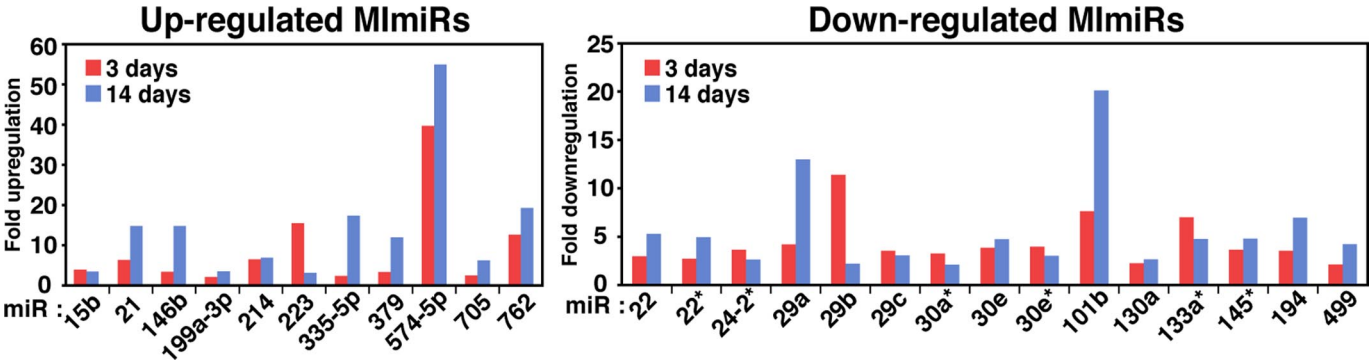

Fig. S1. Bargraph representation of miRs regulated 2 or more fold in the borderzone region of mice both 3 days and 14 days after MI as determined by microarray anlysis. Values are expressed as fold change compared with sham operated animals.

Fig. S2. Homology of miR-29 family members. Sequence alignment of miR-29 family members indicates a conserved seed region (nucleotides 2–8 at the 5′ end) and a high level of sequence conservation in the 3′ end of the miRNAs. Both miR-29b-1 and miR-29a and miR-29b-2 and miR-29c are transcribed from a common pri-miRNA.

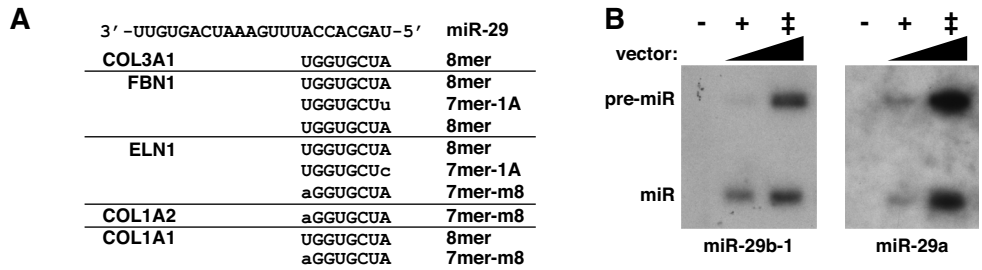

Fig. S3. miR-29 targets mRNAs encoding extracellular matrix proteins. (*A*) Potential binding sites for miR-29 in 3′ UTR's of key fibrotic genes. The seed region of miR-29 (bp 2–8) (depicted in *Upper*) is able to bind complementary reverse to sequences located in the 3′UTR regions of the indicated genes. (*B*) Northern blot analysis on COS cells transfected with increasing amounts of the CMV expression plasmid encoding the miR-29b-1/miR-29a cluster, shows efficient overexpression of miR-29a and miR-29b.

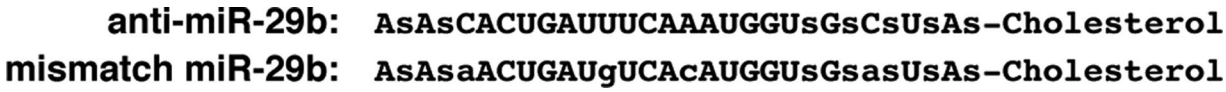

Fig. S4. Chemical structure of cholesterol-modified oligonucleotides complementary to the mature miRNA sequence of miR-29b (anti-miR-29b) or an oligonucleotide containing a four base mismatch antimiR-29 (mm). Each residue is a 2′-OMe modified nucleoside, S is a phosphorothioate internucleoside bond, and − is a hydroxyproline linker.

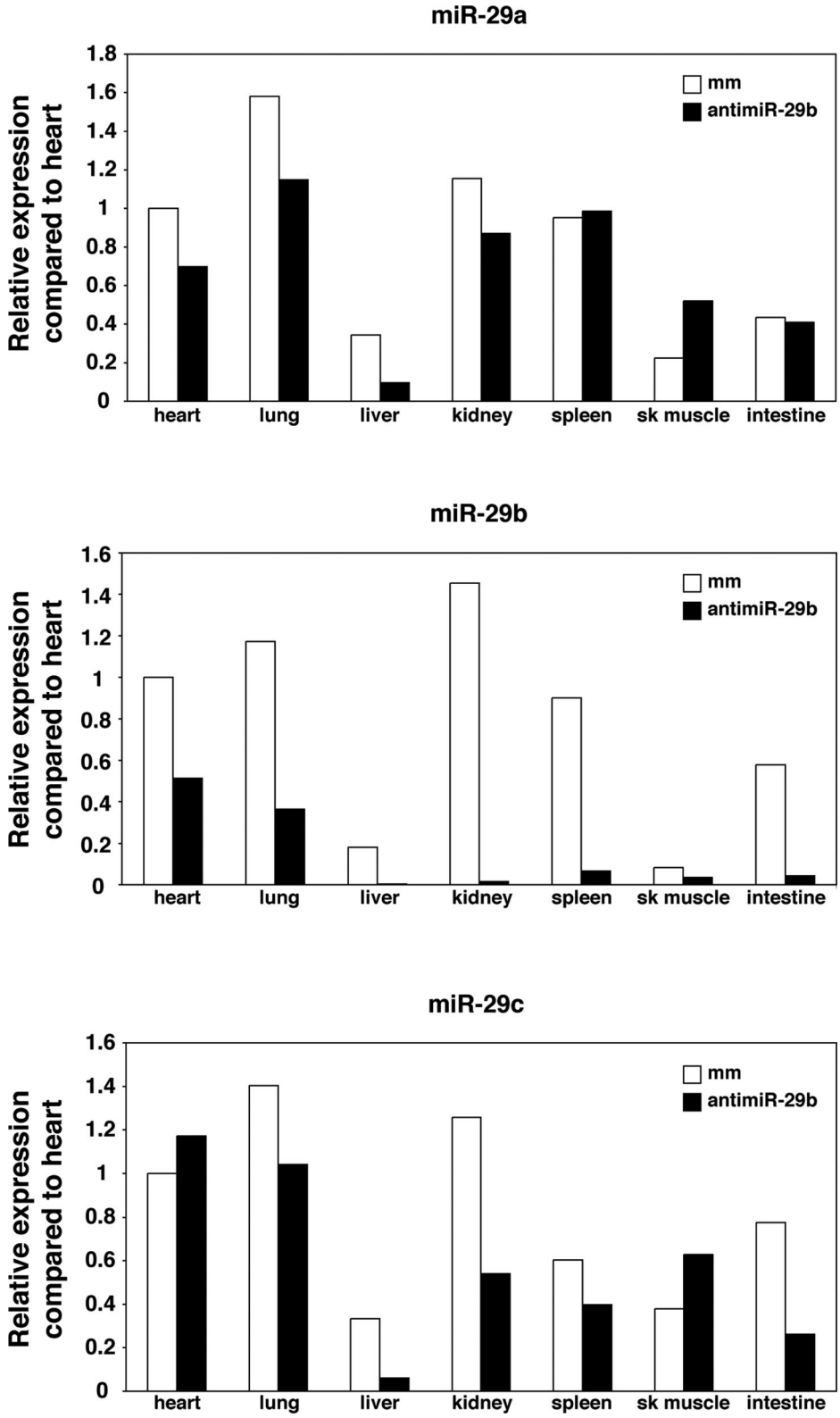

Fig. S5. Knockdown of all miR-29 members in the different tissues indicates that miR-29b shows a 50% reduction in the heart in response to anti-miR-29, whereas miR-29a and -c only show marginal changes. However, the knockdown of miR-29b in liver and kidney in response to anti-miR-29 is almost complete, whereas miR-29a and -c also seem to be reduced in these tissues in response to anti-miR-29b.

Table S1. Significantly up-regulated miRNAs (>2%) in response to MI compared with sham-operated animals. Data are presented as fold change compared with sham-operated

	Border zone of infarcted area		Remote myocardium	
miR	3 days	14 days	3 days	14 days
miR-21	6.3	14.8	2.6	12.6
miR-15b	3.9	3.5		3.4
miR-223	15.5	3.2		6.0
miR-214	6.5	6.9	2.4	
miR-132	3.2			
miR-222	2.8		2.6	
miR-483	6.3			
miR-199a-3p	2.1	3.6		
miR-379	3.3	12.0		
miR-221	2.0			
miR-762	12.6	19.3	2.5	
miR-92b	2.3			
miR-146b	3.5	14.8		6.6
miR-705	2.5	6.2		
miR-574-5p	39.7	54.9		
miR-335-5p	2.4	17.4		12.0
miR-711	19.2			
miR-218		2.1		2.2
miR-739		12.0		5.4
let-7e		41.4		3.1
miR-10b		11.2		10.8
miR-923		19.8		5.9
let-7j		39.9		37.8
miR-199*		4.3		
let-7 g		23.6		21.7
miR-16		9.8		9.8
miR-638		12.2		3.0
miR-10a		8.4		10.3
miR-146a		2.4		
let-7 h		15.3		10.0
miR-26b		2.2		2.1
miR-155		9.5		2.2
miR-352		2.7		2.3
let-7d		2.2		
let-7b		23.1		15.7
miR-365				12.6
miR-34a			2.0	
miR-107			2.0	
miR-103			2.1	
miR 140*		4.2	2.7	
miR-127			2.9	
miR-497			4.7	
miR-199a-5p		10.3	2.8	
miR-199b*		196.9	2.1	

Table S2. Significantly downregulated miRNAs (>2 fold) in response to MI compared with sham-operated animals. Data are presented as fold change compared with sham-operated

	Border zone of infarcted area		Remote myocardium	
miR	3 days	14 days	3 days	14 days
miR-149	11.5			
miR-101b	7.6	20.1		
miR-133a*	7.0	4.8		
miR-101a	7.9			4.3
miR-24-2*	3.7	2.6		
miR-218	4.8		2.1	
miR-126-5p	64.4		67.6	
miR-145*	3.6	4.8		
miR-689	2.1			
miR-22	3.0	5.3		3.6
miR-499	2.1	4.2		
miR-30a*	3.2	2.1	2.0	
miR-22*	2.7	5.0		2.3
miR-192	2.7			
miR-194	3.6	7.0		2.8
miR-29c	3.6	3.1		
miR-30e	3.8	4.7		3.0
miR-130a	2.3	2.7		
miR-181d	3.8		3.2	2.6
miR-100	2.5			
miR-29b	11.4	2.2	2.0	
miR-30e*	4.0	3.0	2.3	
miR-29a	4.2	13.0	2	
miR-690		3.9		2.4
miR-106a		3.1		
miR-17-5p		3.8		2.3
miR-451		2.8		
miR-143		4.0		2.0
miR-34c-3p		89.9		7.7
miR-93		3.9		3.1
miR-30a		2.5		
miR-148a		2.1		
miR-34a		4.4		6.4
miR-106b		4.3		2.3
miR-22b		4.1		2.8
miR-378		3.9		2.7
miR-150		2.9		
miR-128a		3.2		
miR-185		4.0		3.8
miR-139		2.3		
miR-423-5p		2.2		3.0
miR-320		2.0		3.4
miR-20a		3.1		
miR-20b		2.8		
miR-103		2.3		2.2
miR-352			2.2	
miR-155			2.4	
miR-218			2.1	

Table S3. Primers 3′-UTRs predicted target genes miR-29

Fragment	Forward primer	Reverse primer
miR-29b1/29a	GGCCGTGGATGTGTAG	GTGTGTCCAACCTGTGGCC
UTR COL1A1	ACTCCCTCCACCCCAATCTGG	CTGATGCAGGACAGACCAAGAGAGGC
UTR COL1A2	GAGAAGGATTGGTCAGAGCAG	CACACACAATGCACATCAATGTGGAG
UTR COL3A1	GCCAAACTCTCTGAAACCCCAG	GAGTATGACCGTTGCTCTGC
UTR FBN1	TTCACCAUCCAGAGACC	GCGGTGGTGATCCTCTG
UTR ELN1	TCTTCTGGGGACCCCTG	CACCAAATCCATCGTCAAGGC